Development of ^{19}F NMR for Measurement of [Ca^{2+}]$_i$ and [Pb^{2+}]$_i$ in Cultured Osteoblastic Bone Cells

by Francis A. X. Schanne*[†], Terry L. Dowd,[‡] Raj K. Gupta,[‡] and John F. Rosen*

Lead (Pb) has been shown to perturb cellular calcium (Ca) homeostasis, altering sizes and flux rates of cellular pools of exchangeable Ca and impairing Ca-mediated cell processes. To date, however, a direct effect of Pb on intracellular-free Ca^{2+} has not yet been demonstrated. Heavy metals bind to the commonly used fluorescent Ca ion indicators with greater affinity than does Ca and thereby interfere with the expected Ca-dependent fluorescence.

In this study, the fluorinated Ca ion indicator, 1,2-bis(2-amino-5-fluorophenoxy)ethane N,N,N',N'-tetraacetic acid (5F-BAPTA), and ^{19}F NMR were used to measure the free intracellular Ca ion concentration ([Ca^{2+}]$_i$) in the rat osteoblastic bone cell line, ROS 17/2.8. Both Pb and Ca bind to 5F-BAPTA with high affinity, but the Pb-5F-BAPTA comple produces a ^{19}F NMR signal at a chemical shift distinct from 5F-BAPTA and the Ca-5F-BAPTA complex. The apparent dissociation constants for Pb-5F-BAPTA and Ca-5F-BAPTA are 2×10^{-10} M and 5×10^{-7} M, respectively, at 30°C, pH 7.1, and Mg^{2+} (0.5 mM). Thus, this methodology allows for the simultaneous identification and quantification of free Pb and free Ca ion concentrations. Determinations of [Ca^{2+}]$_i$ were based on ^{19}F NMR measurements of 5F-BAPTA-loaded ROS 17/2.8 osteoblastic bone cells that were attached to collagen-coated microcarrier beads. Cells were continuously superfused with freshly oxygenated medium at 30°C. Under these conditions, the [Ca^{2+}]$_i$ of ROS 17/2.8 cells was observed to be 128 ± 14 nM. Treatment with parathyroid hormone produced a nearly 2-fold increase in [Ca^{2+}]$_i$ within the first half hour, with a subsequent return to pretreatment levels. This work demonstrates the usefulness of 5F-BAPTA and ^{19}F NMR for measuring [Ca^{2+}]$_i$ in cells in monolayer culture in response to physiologic agents, and it indicates its potential for studies of the toxic effect of heavy metals on cellular Ca homeostasis.

Introduction

In 1985, the Centers for Disease Control lowered its definition of an elevated blood lead level from 30 to 25 μg/dL in young children (*1*). Current estimates with this standard have indicated that 1.5 to 2.3 million American children have elevated blood lead values (*2,3*), values associated with multiple metabolic (*4*), neurologic (*5,6*), and behavioral disorders (*6,7*). Evidence also continues to accumulate that demonstrates associations between even lower blood lead levels and reductions in mental development (*8*), decreased skeletal growth (*9*) and disturbances in cardiovascular function (*10,11*). One such epidemiologic study, which analyzed data from the Second National Health and Nutrition Examination Survey, revealed a strong negative correlation between blood lead levels and height or skeletal growth in children (*9*).

Interactions between Pb toxicity and Ca metabolism are well recognized, both at the level of the organism as a whole and at the cellular level (*12*). The handling of Ca and Pb by bone cells is given special importance because bone is the major reservoir in the body for both the essential metal Ca and the toxic metal Pb. A comprehensive basis on which to access the possible sites where Pb might interfere with Ca homeostasis at the cellular level can be derived from ^{45}Ca desaturation kinetic techniques. Pounds and Rosen, using this methodology, described the steady-state homeostasis of Ca in primary cultures of murine osteoclastic bone cells as consisting of three distinct intracellular compartments of exchangeable Ca (*13*). They found that adding increasing concentrations of Pb to the extracellular medium resulted in elevations in all three intracellular compartments. The largest

Departments of *Pediatrics, [†]Pathology, and [‡]Physiology and Biophysics, Albert Einstein College of Medicine, Montefiore Medical Center, Bronx, NY 10467.

Address reprint requests to F. A. X. Schanne, Montefiore Medical Center, Department of Pediatrics, 111 East 210th Street, Bronx, NY 10467.

increase occurred in the most slowly exchanging compartment that includes the mitochondrial calcium.

In virtually every tissue where the effects of lead were studied in detail, the results suggested that lead alters calcium homeostasis and calcium-mediated cell function. In nerve (14,15), smooth muscle (16), cardiac muscle (17), liver (16,19), and bone cells (13,20), the hypothesis has been proposed that lead causes an increase in intracellular pools of calcium and a decrease in the ability of cells to extrude calcium or lower the effective free intracellular calcium ion concentrations $[Ca^{2+}]_i$.

The appropriate temporal and spatial availability of intracellular Ca is critical to the modulation of cellular structure, function, and activity. Given the central role of $[Ca^{2+}]_i$ in the regulation of cellular processes, we propose that an early, discrete, yet common event in the mechanism of low-level lead toxicity is the inappropriate elevation and regulation of $[Ca^{2+}]_i$, leading to an important subset of the variety and magnitude of disorders associated with lead toxicity.

In order to directly test this hypothesis, $[Ca^{2+}]_i$ must be measured in a target tissue of Pb effects; and $[Ca^{2+}]_i$ dynamics must also be measured in response to normal physiologic calciotropic agents and to Pb treatment. Testing this hypothesis requires a methodology that can measure $[Ca^{2+}]_i$ in the presence of Pb. The commonly used fluorescent Ca indicators Quin-2, Fura-2 and Indo-1 bind heavy metals with greater specificity than they do Ca (21,22). It has thus far proven difficult, if not impossible, to dissociate fluorescence changes that reflect actual changes in $[Ca^{2+}]_i$ from those reflecting the binding of heavy metals (22,23), without specifically removing the heavy metals from the cells being studied (22). Pb has also been shown to trigger luminescence of the photoprotein Ca indicator, aequorin (24,25), thereby eliminating it as an alternative $[Ca^{2+}]_i$ indicator in these studies.

While the high-affinity binding of heavy metals is a major drawback for the fluorescent and bioluminescent indicators, it represents a major advantage for the 5,5'difluoro derivative of 1,2-bis(2-aminophenoxy)ethane-N,N,N',N'-tetraacetic acid (5F-BAPTA) (26). BAPTA, the predecessor of Quin-2 and Fura-2, symmetrically substituted with fluorine at the 5 position of the two rings, is a cation indicator that can be monitored by ^{19}F nuclear magnetic resonance spectroscopy (^{19}F NMR). The ^{19}F chemical shift of this compound is highly sensitive to chelation with metal ions (M^{n+}). These ^{19}F chemical shifts are characteristic and distinct for 5F-BAPTA and each M^{n+}-5F-BAPTA complex thus far described (26). Furthermore, the areas of the resonances from the bound (M^{n+}-5F-BAPTA) and free (5F-BAPTA) forms of the indicator are proportional to their concentrations, and the free M^{n+} concentration can be calculated by knowing the dissociation constant for M^{n+}-5F-BAPTA. Thus, ^{19}F NMR permits the identification and quantitation of each chelated ion. Metcalfe and

co-workers have successfully employed this methodology to simultaneously monitor changes in $[Ca^{2+}]_i$ and intracellular $[Zn^{2+}]$ (27).

In testing our hypothesis, it is appropriate to choose a cell that is a target of low-level Pb toxicity. Osteocalcin, the vitamin K-dependent protein found in bone matrix, is a specific biochemical marker of osteoblastic activity and can be measured in the serum. Markowitz, Gundberg and Rosen (28) observed that in lead-toxic children, those with the highest body burden of Pb had the lowest osteocalcin levels. Successful reduction of body Pb stores by $CaNa_2EDTA$ chelation therapy ultimately resulted in marked elevations in circulating osteocalcin levels. Although regulation of osteoblastic activity is multifactorial, these data suggest that Pb either directly or indirectly impairs osteoblastic activity. Such toxic effects on osteoblastic function could also explain the observed negative correlation between skeletal growth and blood Pb values in children (9).

For our experiments, we have chosen the rat osteoblastic osteosarcoma cell line, ROS 17/2.8. The ROS 17/2.8 cell is well characterized, highly differentiated, and phenotypically an osteoblast (29). These cells synthesize osteocalcin, have high alkaline phosphatase activity, possess 1,25-dihydroxyvitamin D_3 receptors, and respond to parathyroid hormone (PTH) by increasing adenylate cyclase activity (29) and elevating $[Ca^{2+}]_i$ (30). The responsiveness of these cells to PTH allows us to assess the usefulness of our $[Ca^{2+}]_i$ indicator in monitoring the normal response of these cells to a physiologic calciotropic hormone.

Methods

Cell Culture

ROS 17/2.8 cells were maintained and grown to confluence in 75-cm^2 flasks with Ham's F-12 nutrient mixture supplemented with 5% fetal bovine serum and 28 mM HEPES buffer, pH 7.4 (F-12 medium). Two days before NMR observations were made, the ROS 17/2.8 cells were harvested by trypsinization (0.01% in Ca^{2+}-Mg^{2+}-free Hank's balanced salt solution) and attached to collagen-coated microcarriers (Cytodex 3, Pharmacia), which had been swollen in saline and equilibrated in F-12 medium. One hundred twenty million cells were seeded onto 8 mL of swollen beads (approximately 0.6 g dry wt). Upon attachment and flattening, complete confluence was achieved within 24 hr. ROS 17/2.8 cells on beads were maintained in 500 mL of F-12 medium in a 1-L siliconized glass, Techne stir vessel at 35 rpm, 37°C, 95% air, 5% CO_2, humidified atmosphere. The medium was changed twice daily.

Loading with 5F-BAPTA

Cells were loaded with 5F-BAPTA in the stirring culture flask for 45 min. This was done by adding the

acetoxymethyl ester of 5F-BAPTA at a concentration of 20 μm from a 50-mM stock solution in dimethyl-sulfoxide. The loading medium was removed, the cells were washed in fresh F-12 medium and were allowed 1 hr to recover from loading. Next, cells on beads were transferred to a 10-mm diameter NMR tube. An inflow tubing line was inserted down through the beads to the bottom of the NMR tube, and an outflow tubing line was inserted to the top of the NMR tube. The NMR tube was sealed with a rubber stopper and the F-12 medium, saturated with 95% O_2, 5% CO_2, was superfused through the NMR tube at a rate of 2 mL/min, discarding the effluent. The NMR samples were maintained at 30°C throughout the signal accumulation (Fig. 1).

NMR

NMR measurements of 5F-BAPTA-loaded cells were performed on a Varian 500 MHz spectrometer using a 10-mm broad band probe. The decoupler coil, used to observe the ^{19}F resonance, was tuned to 470.268 MHz. NMR parameters were as follows: acquisition time, 0.8 sec; pulse angle, 90°; and spectral width, 10 KHz. Each spectrum represented the Fourier transformation of the sum of 2500 free induction decays (FID) over a time interval of 33.3 min

Each experiment was begun by acquiring three consecutive spectra in order to establish baseline $[Ca^{2+}]_i$ in untreated cells. Treatments were initiated by addition to the superfusion medium. NMR measurements of standard aqueous solutions, performed to determine M^{n+}-5F-BAPTA chemical shifts and apparent binding constants, were also performed on the Varian 500 MHz spectrometer; but a 5-mm diameter tube and a dedicated fluorine probe were used.

^{31}P NMR spectra of ROS 17/2.8 cells were also obtained on the Varian 500 MHz spectrometer operating at 202.3 MHz for phosphorous-31. The NMR parameters were: acquisition time, 0.8 sec; pulse angle, 90°; spectral width, 20 KHz, and a recycle time of 1.6 sec. Each spectrum represented the Fourier transformation of the sum of 8,000 transients, using a line-broadening function of 50 Hz. The intracellular

pH of the cells was determined based on the chemical shift difference between the intracellular inorganic phosphate (P_i) and phosphocreatine (PCR) peaks as previously described (*31*), and was found to be 7.1. The intracellular-free Mg^{2+} concentration was determined based on the chemical shift difference between the P_α and P_β peaks of ATP (*32*), and was found to be 0.5 mM. The intracellular volume was estimated based on phenotypic morphology (*29*).

Apparent Dissociation Constants

The K_d for Ca-5F-BAPTA was determined under the following conditions: KCl (135 mM), $MgCl_2$ (0.5 mM), K_4-5F-BAPTA (0.385 mM), MOPS buffer (10 mM), pH 7.1, 30°C and varying amounts of $CaCl_2$. Free Ca^{2+} concentrations were measured by using a Ca^{2+}-selective ion electrode (Orion) that was calibrated with Ca-EDTA standards. The intensities of Ca-5F-BAPTA and 5F-BAPTA resonances, which are proportional to their concentrations, were measured using the areas under their respective ^{19}F peaks. The electrode-determined free Ca^{2+} concentration was plotted verses the ratio of the bound-to-free 5F-BAPTA, yielding the K_d as the slope. The K_d for Pb-5F-BAPTA was determined by competition with Ca^{2+}.

Materials

ROS 17/2.8 cells were a generous gift from Dr. G. A. Rodan (Merck Sharp and Dohme, West Point, PA). 5F-BAPTA and its acetoxymethyl ester (AME) were synthesized by Dr. Iraj Lalezari by previously described methods (*33*). Synthetic bovine PTH (*1-34*) was obtained from Sigma (St. Louis, Mo). Collagen-coated microcarriers (Cytodex 3) were obtained from Pharmacia (Uppsala, Sweden).

Results and Discussion

The purpose of this report is to describe and determine the potential usefulness of 5F-BAPTA and ^{19}F NMR as a methodology for measuring $[Ca^{2+}]_i$ in a single population of cells in monolayer culture during treatment with Pb. Several criteria must be met in order to demonstrate the usefulness of this technique. First, the technique must be able to distinguish and measure $[Ca^{2+}]_i$ in the presence of Pb. The indicator 5F-BAPTA must be taken up and trapped within the cells in sufficient quantity to yield a clearly observable ^{19}F NMR signal. This must be achieved without producing permanent alterations in cellular energetics and ion balances. Moreover, the methodology must prove effective in monitoring normal changes in $[Ca^{2+}]_i$, such as those produced by physiologic, calciotropic hormones.

Figure 2 represents the ^{19}F NMR spectrum of a solution that contained $K_4$5F-BAPTA (0.52 mM), $MgCl_2$ (0.5 mM), $ZnSO_4$ (0.13 mM), Pb $(C_2H_3O_2)_2$ (0.13
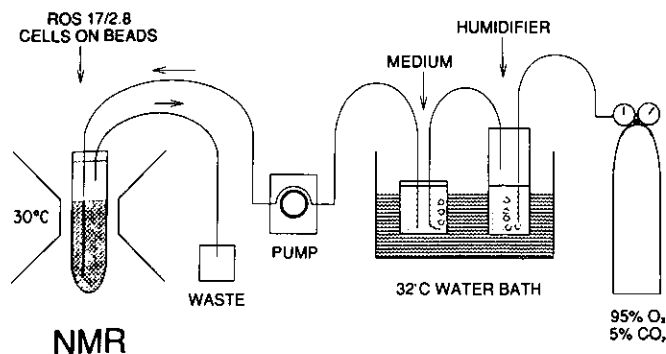

FIGURE 1. Schematic of superfusion system for maintaining ROS 17/2.8 cells attached to Cytodex #3 microcarrier beads while in the NMR spectrometer.
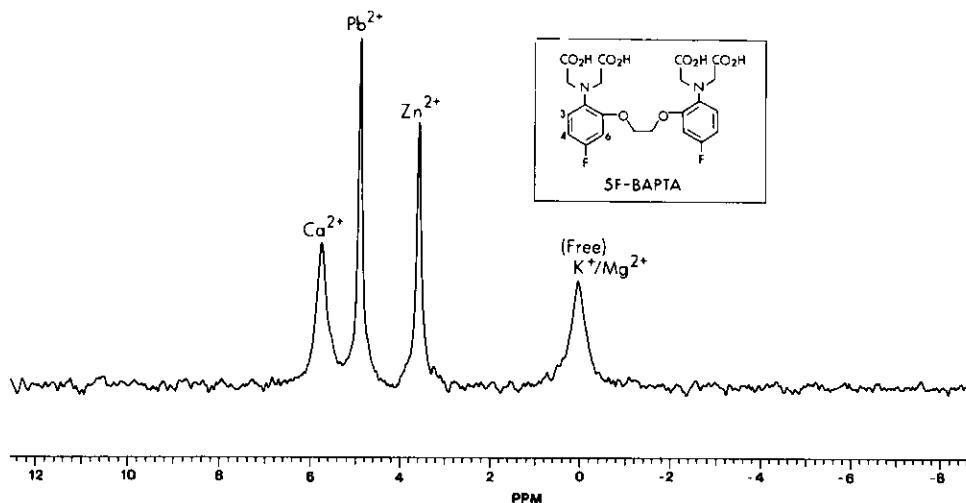
FIGURE 2. ^{19}F NMR spectrum of 5F-BAPTA (0.52 mM) in aqueous solution with MgCl$_2$ (0.5 mM), ZnSO$_4$ (0.13 mM), Pb(C$_2$H$_3$O$_2$)$_2$ (0.13 mM), CaCl$_2$ (0.13 mM), KCl (135 mM), MOPS (10 mM), pH 7.1. at 30°C and 470.268 MHz. The resonance peaks are as indicated for free 5F-BAPTA (K+, Mg^{2+}) and each M^{n+}-5F-BAPTA complex (Ca^{2+}, Pb^{2+}, Zn^{2+}). Inset represents the structure of 5F-BAPTA.

mM), CaCl$_2$ (0.13 mM), KCl (135 mM), and MOPS (10 mM) with a pH 7.1 at 30°C. This spectrum illustrated the relative ^{19}F chemical shifts for 5F-BAPTA and its complexes with Zn and Ca that are consistent with those originally described by Smith et al. (24). Furthermore, this spectrum clearly demonstrated a distinct chemical shift for Pb-5F-BAPTA. This Pb-5F-BAPTA peak fell between the peaks of Ca and Zn bound complexes, 0.8 ppm upfield from the Ca-5F-BAPTA resonance. The free 5F-BAPTA was in rapid exchange with Mg^{2+} complex so that the latter does not give rise to a distinct resonance, rather it merely results in a broadening of the free 5F-BAPTA resonance (24). With the K_d for Mg-5F-BAPTA in the range of 17 mM (24,33), the amount of free 5F-BAPTA bound to Mg^{2+} at 0.5 mM was approximately 3%. In order to fully compensate for the slight association of Mg^{2+} with the 5F-BAPTA, all apparent binding constants were determined in the presence of 0.5 mM MgCl$_2$, the [Mg^{2+}]$_i$ of ROS 17/2.8 cells, as determined by ^{31}P NMR.

Determination of the K_d for Ca-5F-BAPTA under these conditions was based on the free [Ca^{2+}]$_i$ versus the ratio of the Ca^{2+} bound to free forms of the chelator measured by ^{19}F NMR. The K_d for Ca-5F-BAPTA was 5.0 ± 0.2 x 10^{-7} M (mean ± SEM, n = 8). This value is similar to those reported by Smith et al. (26) and Levy et al. (34), especially accounting for differences in temperature and Mg concentration, but nearly twice that reported by Marban et al. (35).

Determination of the K_d for Pb-5F-BAPTA was based on competition between Pb and Ca for binding to 5F-BAPTA and was measured by ^{19}F NMR. This yielded a K_d of 2.1 ± 0.5×10^{-10} M (mean ± SEM, n = 4) for Pb-5F-BAPTA. The determination of the specific, characteristic chemical shifts for both Ca-5F-BAPTA and Pb-5F-BAPTA, as well as their apparent K_ds, would thereby permit the simultaneous identification and measurement of both [Ca^{2+}] and [Pb^{2+}] by this technique.

Figure 3 represents a typical ^{19}F NMR spectrum from control, untreated ROS 17/2.8 cells on microcarrier beads. The cells were loaded with 5F-BAPTA. ROS 17/2.8 cells were superfused with medium at 2 mL/min at 30°C in an NMR tube for an additional hour to achieve equilibrium. The free 5F-BAPTA peak was set at 0 ppm with the resonance of Ca-5F-BAPTA complex located 5.7 ppm downfield. These were consistent with their identification in Figure 2. Figure 3 illustrates two clearly distinct, definable, and measurable ^{19}F resonance signals from which the ratio of free-to-bound forms of 5F-BAPTA was determined. This ratio, together with the measured K_d, yielded [Ca^{2+}]$_i$ of untreated ROS 17/2.8 cells of 128 ± 14 nM (mean ± SD, n = 10).

The total 5F-BAPTA trapped within cells was approximately 0.5 mM. This determination was based on the total ^{19}F signal measured during the initial FID accumulation interval, compared to 5F-BAPTA concentration standards. The total ^{19}F signal was measured at each 33.3 min accumulation interval throughout the course of all experiments, each of which lasted 5 to 7 hr. Based on the ^{19}F signal measured at each interval, there was an apparent first-order rate of loss of 5F-BAPTA of 12%/hr. It must be noted that these cells were being superfused with medium at a rate of 2 mL/min. Thus, any 5F-BAPTA that leaked from the cells was constantly being diluted and washed away, thereby contributing less than 0.5% to the ^{19}F signal in any given accumulation interval. Despite this constant loss of intracellular indicator, there were no concurrent changes in the [Ca^{2+}]$_i$ measured in the cells during the time course of the NMR experiments. Therefore, while 5F-BAPTA may act as a major intracellular Ca^{2+} buffer, its concentration did not alter the steady state [Ca^{2+}]$_i$, which was consistent with the findings of Murphy et al. in red blood cells (36).
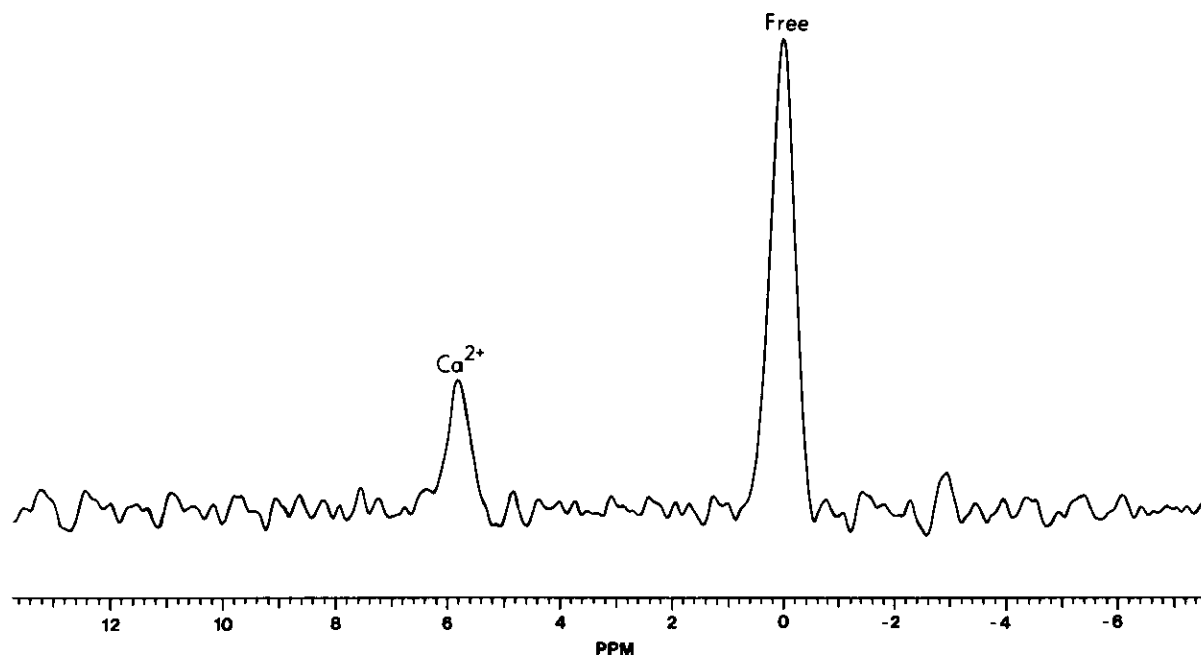
FIGURE 3. ¹⁹F NMR spectrum of ROS 17/2.8 cells on microcarrier beads which had been loaded with 5F-BAPTA and allowed to equilibrate. Superfusion was carried out at 30 °C with F-12 medium (2 mL/min) in a 10-mm diameter NMR tube. The free 5F-BAPTA and the Ca-5F-BAPTA complex (Ca²⁺) are identified.

In order to assess the viability, metabolic integrity, and ion balance of ROS 17/2.8 cells following their loading with 5F-BAPTA, a ³¹P spectrum was obtained. Figure 4 represents the ³¹P spectrum of ROS 17/2.8 cells loaded with 5F-BAPTA. The large resonance toward the left end of the spectrum represented the extracellular inorganic phosphate (P_i), which was 1 mM in the medium. The phosphocreatine (PCR) and the P_α, P_β, and P_γ resonance peaks of ATP were also identified. ³¹P spectra were obtained to quantitate several critical indicators of cellular functioning: a) the size of the P_β resonance of ATP is proportional to the cellular ATP concentration (37); b) the intracellular pH was determined based on the chemical shift difference between the intracellular P_i and PCR peaks (31); and c) the [Mg²⁺]ᵢ was determined

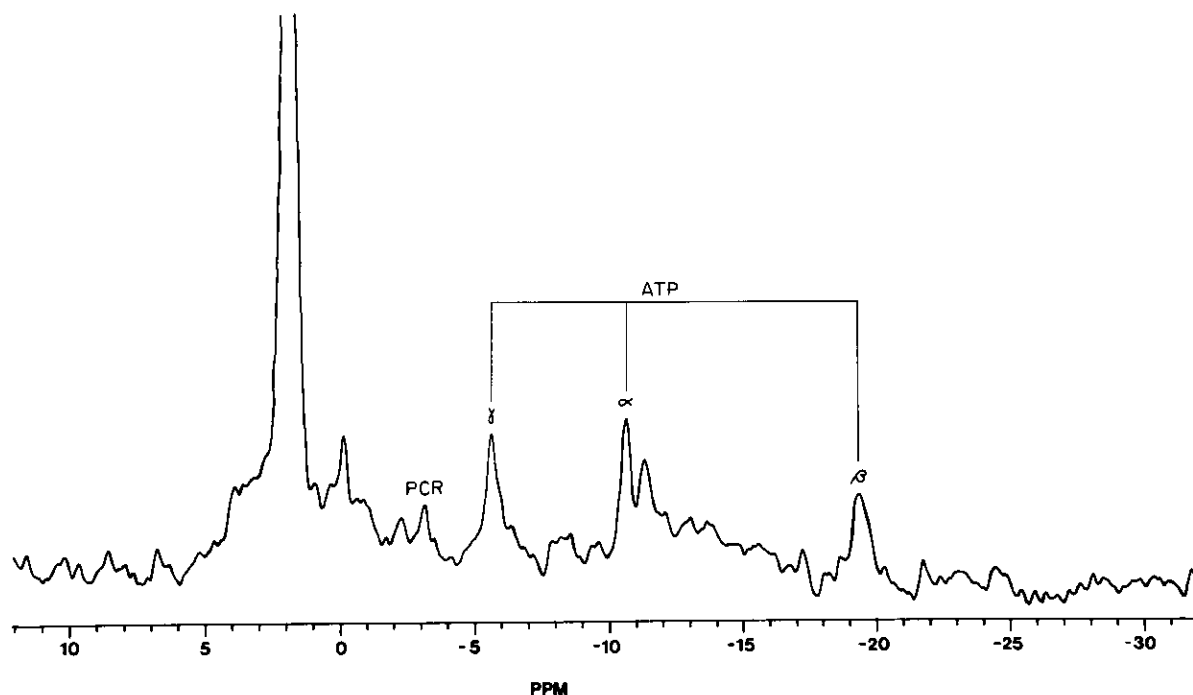FIGURE 4. ³¹P NMR spectrum of ROS 17/2.8 cells treated as in Figure 3. The large resonance toward the left of the spectrum represents extracellular inorganic phosphate. Phosphocreatine (PCR) and the P_α, P_β, and P_γ resonance peaks of ATP are identified.

based on the chemical shift difference between the P_α and P_β resonance peaks of ATP (*32*).

Under our conditions of loading, recovery and superfusion, there was virtually no observable difference in the ^{31}P NMR spectrum of ROS 17/2.8 cells, which had been loaded with 5F-BAPTA, compared to those which had not been loaded with respect to ATP level, intracellular pH, and $[Mg^{2+}]_i$. These findings indicated that 5F-BAPTA loading appeared to have left ROS 17/2.8 cells intact in terms of viability, metabolic integrity, and ionic balance.

Finally, this technique was used to study the response of ROS 17/2.8 cells to hormonal stimulation. Figure 5 shows ^{19}F spectra, which demonstrate the response of ROS 17/2.8 cells to treatment with PTH (400 ng/mL). Panel *A* represents untreated ROS 17/2.8 cells, as seen in Figure 3, but immediately before addition of PTH. The $[Ca^{2+}]_i$ was 130 nM. Panel *B* represents the ^{19}F spectrum accumulated during the first 33 min after addition of PTH. $[Ca^{2+}]_i$ had rise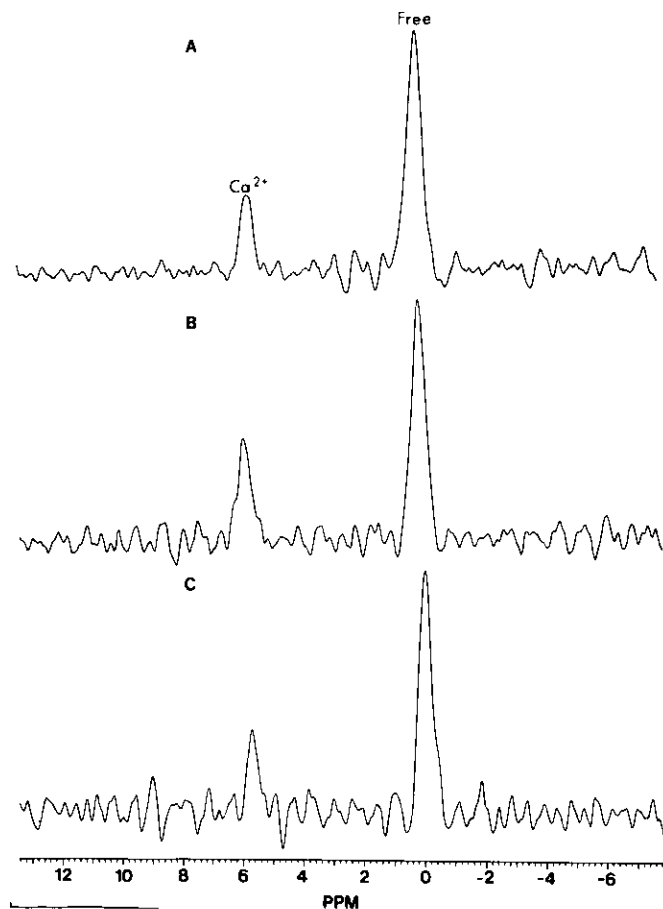n to 240 nM. Panel *C* represents the ^{19}F signal during washout of PTH, which followed 100 min of treatment. During this time period, the $[Ca^{2+}]_i$ had fallen to 140 nM or near pretreatment levels. These spectra illustrated changes in the size of the Ca-5F-BAPTA ^{19}F resonance, as compared to the free 5F-BAPTA in response to PTH treatment. The full time course of changes in $[Ca^{2+}]_i$ in response to PTH, as monitored by ^{19}F NMR, is illustrated in Figure 6. These data showed the responsiveness of ROS 17/2.8 cells to hormonal stimulation, as evidenced by an anticipated rise in $[Ca^{2+}]_i$, which is consistent with the findings of Yamaguchi et al. (*30*).

Conclusions

This report describes the usefulness of 5F-BAPTA and ^{19}F NMR as a methodology for measuring $[Ca^{2+}]_i$ in ROS 17/2.8 osteoblastic bone cells in monolayer culture. The cells were grown to confluence and maintained on collagen-coated microcarriers and were subsequently loaded with 5F-BAPTA to yield clearly observable ^{19}F NMR spectra, which were used to determine the $[Ca^{2+}]_i$. Loading with 5F-BAPTA occurred without producing irreversible alterations in cellular functioning, demonstrated by ATP levels, intracellular pH, $[Mg^{2+}]_i$, and hormonal responsiveness to PTH. 5F-BAPTA and ^{19}F NMR have proven effective in measuring changes in $[Ca^{2+}]_i$ in response to this calciotropic hormone.

The time intervals required to accumulate sufficient signal intensity for accurate measurements of $[Ca^{2+}]_i$ were considerably longer than those for more commonly used indicators such as Quin-2, Fura-2 and aequorin. However, these results demonstrate the advantage of using NMR for studying cells under long-term stable conditions, such as our oxygenated superfused monolayer cultures.
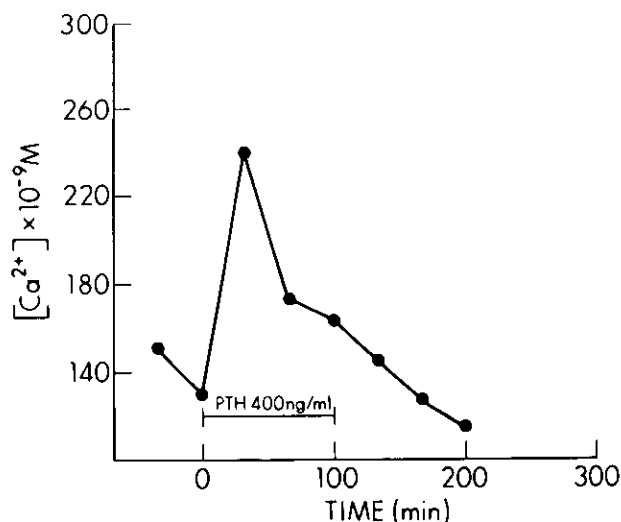

FIGURE 5. ^{19}F NMR spectra of 5F-BAPTA loaded ROS 17/2.8 cells before (*A*), during (*B*), and after (*C*) treatment with PTH (400 ng/mL). Panel *A* represents ^{19}F signal accumulation interval immediately before treatment with PTH. Panel *B* represents ^{19}F signal accumulation after addition of PTH. Panel *C* represents ^{19}F signal accumulation during washout of PTH following 100 min of treatment. Each ^{19}F signal accumulation interval required 33.3 min.

FIGURE 6. Time course of change in $[Ca^{2+}]_i$ in ROS 17/2.8 cells in response to PTH treatment.

This technique provides for monitoring long-term steady-state changes in $[Ca^{2+}]_i$ that may occur in response to hormonal stimulation or toxic insult. These changes are distinct from the rapid changes more readily measured using the fluorescent and chemoluminescent Ca^{2+} indicators. Furthermore, the demonstration that 5F-BAPTA and ^{19}F NMR can selectively identify and measure concentrations of both Ca^{2+} and Pb^{2+} simultaneously indicates the potential for these methods to be used in toxicological studies of the effects of Pb and other heavy metals on intracellular $[Ca^{2+}]$ homeostasis.

NOTE ADDED IN PROOF: Using this methodology, we have recently described a Pb-induced sustained elevation in $[Ca^{2+}]_i$ and detected $[Pb^{2+}]_i$ in ROS 17/2.8 cells (*38*).

REFERENCES

1. Preventing Lead Poisoning in Young Children. A Statement by the Centers for Disease Control, Atlanta, GA, 1985.
2. Piomelli, S., Rosen, J. F., Chisolm, J. J., and Graef, J. Management of childhood lead poisoning. J. Peds. 105: 523-532 (1984).
3. National Center for Health Statistics. Blood lead levels for persons ages 6 months-74 years: United States, 1976-1980. U.S. Dept. of Health and Human Services, Hyattsville, MD., 1984.
4. Rosen, J. F. Metabolic and cellular effects of lead: a guide to low level lead toxicity in our children. In: Dietary and Environmental Exposure to Lead (K. R. Mahaffey, Ed.), Elsevier/North Holland Biomedical Press, Amsterdam, 1985, pp. 157-185.
5. Needleman, H. L. (Ed.). Low Level Lead Exposure: The Clinical Implications of Current Research. Raven Hill, New York, 1980.
6. Davis, J. M., and Svendsgaard, D. J. Lead and child development. Nature 329: 297-300 (1987).
7. Winneke, G., Kramer, U., Brockhaus, A., Ewers, U., Kaganek, G., Lechner, H., and Janke, W. Neuropsychological studies in children with elevated tooth-lead concentrations. Extended study. Int. Arch. Occup. Environ. Health 51: 232 (1983).
8. Bellinger, D., Leviton, A., Waternaux, C., Needleman, H., and Rabinowitz, M. Longitudinal analyses of prenatal and postnatal lead exposure and early cognitive development. New Engl. J. Med. 316: 1037-1043 (1987).
9. Schwartz, J., Angle, C., and Pitcher, H. Relationship between childhood blood lead levels and stature. Pediatrics 77: 281-288 (1986).
10. Harlan, W. R., Landis, R., Schmouder, R. L., Goldstein, N. G., and Harlan, L. C. Blood lead and blood pressure: Relationship in the adolescent and adult US population. J. Am. Med. Assoc. 253: 530-534 (1985).
11. Pirkle, J. L., Schwartz, J., Landis, J. R., and Harlan, W. R. The relationship between blood lead levels and blood pressure and its cardiovascular risk implications. Amer. J. Epidemiology 121: 246-258 (1985).
12. Pounds, J. G. Effect of lead intoxication on calcium homeostasis and calcium-mediated cell function: a review. Neurotoxicology 5: 295-332 (1984).
13. Rosen, J. F. and Pounds, J. G. Quantitive interactions between Pb^{2+} and Ca^{2+} homeostasis in cultured osteoclastic bone cells. Toxicol. Appl. Pharmacol. 98: 530-543 (1989).
14. Cooper G. P., Suszkiw, J. B., and Manalis, R. S. Heavy metals: effects on synaptic transmission. Neurotoxicology 5: 247-266 (1984).
15. Atchison, W. D., and Narahashi, T. Mechanism of action of lead on neuromuscular junctions. Neurotoxicology 5: 267-282 (1984).
16. Webb, R. C., Winquist, R. J., Victery, W., and Vander, A. J. *In vivo* and *in vitro* effects of lead on vascular reactivity in rats. Am. J. Physiol. 241: 211-216 (1981).
17. Kopp, S. J., Glonek, T., Erlanger, M., Perry, E. F., Perry, H. M., and Barany, M. Cadmium and lead effects on myocardial function and metabolism. J. Environ. Pathol. Toxicol. 4: 205-227 (1980).
18. Pounds, J. G., Wright, R., Morrison, D., and Casciano, D. A. Effect of lead on calcium homeostasis in the isolated rat hepatocyte. Toxicol. Appl. Pharmacol. 63: 389-401 (1982).
19. Pounds, J. G., Morrison, D., Wright, R., Casciano, D. A., and Shaddock, J. G. Effect of lead on calcium-mediated cell function in the isolated rat hepatocyte. Toxicol. Appl. Pharmacol. 63: 402-408 (1982).
20. Rosen, J. F. The metabolism of lead in isolated bone cell population: interactions between lead and calcium. Toxicol. Appl. Pharmacol. 71: 101-112 (1983).
21. Grynkiewicz, G., Poenie, M., and Tsien, R. Y. A new generation of Ca^{2+} indicators with greatly improved fluorescence properties. J. Biol. Chem. 260: 3340-3450 (1985).
22. Arslan, P., DiVirgilio, F., Beltrame, M., Tsien, R. Y., and Pozzan, T. Cytosolic Ca^{2+} homeostasis in Ehrlich and Yoshida carcinomas. J. Biol. Chem. 260: 2719-2727 (1985).
23. Conner, J. A. Digital imaging of free calcium changes and of spatial gradients in growing processes in single, mammalian central nervous system cells. Proc. Natl. Acad. Sci. (U.S.) 83: 6179-6183 (1986).
24. Izutsu, K. T., Felton, S. P., Siegel, I. A., Yoda, W. T., and Chen, A. C. N. Aequorin: its ionic specificity. Biochem. Biophys. Res. Commun. 49: 1034-1039 (1972).
25. Shimomura, O., and Johnson, F. H. Further data on the specificity of aequorin luminescence to calcium. Biochem. Biophys. Res. Commun. 53: 490-494 (1973).
26. Smith, G. A., Hesketh, R. T., Metcalfe, J. C., Feeney, J., and Morris, P. G. Intracellular calcium measurements by ^{19}F NMR of fluorine-labeled chelators. Proc. Natl. Acad. Sci. (U.S.) 80: 7178-7182 (1983).
27. Metcalfe, J. C., Hesketh, T. R., and Smith, G. A. Free cytosolic Ca^{2+} measurements with fluorine labelled indicators using ^{19}FNMR. Cell Calcium 6: 183-195 (1985).
28. Markowitz, M. E., Gundberg, C. M., and Rosen, J. F. Sequential osteocalcin (Oc) sampling as a biochemical marker of the success of treatment in moderately lead (Pb) poisoned children. Ped. Res., in press.
29. Rodan, G. A., and Rodan, S. B. Expression of the osteoblastic phenotype. In: Bone and Mineral Research, Annual 2 (W. A. Peck, Ed.), Elsevier Science Publishers, Amsterdam, 1983, pp. 244-285.
30. Yamaguchi, D. T., Hahn, T. J., Iida-Klein, A., Kleeman, C. R., and Muallem, S. Parathyroid hormone-activated calcium channels in an osteoblast-like clonal osteosarcoma cell line. J. Biol. Chem. 262: 7711-7718 (1987).
31. Moore, R. D., and Gupta, R. K. Effect of insulin on intracellular pH as observed by ^{31}P NMR spectroscopy. Intl. J. Quant. Chem., Quant. Biol. Symp. 7: 83-92 (1980).
32. Gupta, R. K., Gupta, P., and Moore, R. D. NMR studies of intracellular metal ions in intact cells and tissues. Ann. Rev. Biophys. Bioeng. 13: 221-246 (1984).
33. Tsien, R. Y. New calcium indicators and buffers with high selectivity against magnesium and protons: design, synthesis, and properties of prototype structures. Biochemistry 19: 2396-2404 (1980).
34. Levy, L. A., Murphy, E., and London, R. E. Synthesis and characterization of ^{19}F NMR chelators for measurement of cytosolic free Ca. Am. J. Physiol. 252: C441-C449 (1987).

35. Marban, E., Kitakaze, M., Kusuoka, H., Porterfield, J. K., Yue, D. T., and Chacko, V. P. Intracellular free calcium concentration measured with ^{19}F NMR spectroscopy in intact ferret hearts. Proc. Natl. Acad. Sci. (U.S.) 84: 6005-6009 (1987).

36. Murphy, E., Levy, L., Berkowitz, L. R., Orringer, E. P., Gabel, S. A., and London, R. E. Nuclear magnetic resonance measurement of cytosolic free calcium levels in human red blood cells. Am. J. Physiol. 251: C496-C504 (1986).

37. Yushok, W. D., and Gupta, R. K. Phosphocreatine in Ehrlich ascites tumor cells detected by non-invasive ^{31}P NMR spectroscopy. Biochem. Biophys. Res. Commun. 95: 73-81 (1980).

38. Schanne, F. A. X., Dowd, T. L., Gupta, R. K., and Rosen, J. F. Lead increases free Ca^{2+} concentration in cultured osteoblastic bone cells: simultaneous detection of intracellular free Pb^{2+} by ^{19}F NMR. Proc. Natl. Acad. Sci. (U.S.) 86: 5133-5135 (1989).